European Journal of Pharmaceutics and Biopharmaceutics 76 (2010) 189–199

Contents lists available at ScienceDirect

European Journal of Pharmaceutics and Biopharmaceutics

journal homepage: www.elsevier.com/locate/ejpb

Research Paper

Rivastigmine-loaded PLGA and PBCA nanoparticles: Preparation, optimization, characterization, *in vitro* and pharmacodynamic studies

Shrinidh A. Joshi, Sandip S. Chavhan, Krutika K. Sawant *

TIFAC Centre of Relevance and Excellence, Centre of PG studies and Research, Pharmacy Department, The Maharaja Sayajirao University of Baroda, Donors Plaza, Fatehgunj, Vadodara 390002, Gujarat, India

ARTICLE INFO

Article history:
Received 5 March 2010
Accepted in revised form 8 July 2010
Available online 15 July 2010

Keywords:
Rivastigmine tartrate
PLGA nanoparticles
PBCA nanoparticles
Factorial design
In vitro release
Morris Water Maze Test

ABSTRACT

Sustained release nanoparticulate formulations of Rivastigmine tartrate (RT) were prepared, optimized (using factorial design) and characterized using the biodegradable polymers, PLGA and PBCA as carriers. The pharmacodynamic performances of the nanoparticles (NPs) were evaluated for brain targeting and memory improvement in scopolamine-induced amnesic mice using Morris Water Maze Test. PLGA NPs were prepared by nanoprecipitation technique, while PBCA NPs were prepared by emulsion polymerization technique. Effect of key formulation variables on particle size (PS) and percentage drug entrapment (PDE) of NPs was studied by using factorial design. PLGA NPs showed PS of 135.6 ± 4.2 nm and PDE of 74.46 ± 0.76 %, whereas PBCA NPS showed PS of 146.8 ± 2.6 nm and PDE of 57.32 ± 0.91%. FTIR and GPC characterization confirmed complete polymerization of *n*-butyl cyanoacrylate (nBCA) monomer into PBCA. DSC thermograms indicated that RT was dispersed as amorphous state in both PLGA and PBCA NPs. TEM studies indicated that the NPs were spherical. *In vitro* studies showed 30.86 ± 2.07% and 43.59 ± 3.80% release from PLGA and PBCA NPs in 72 h, respectively. Pharmacodynamic study demonstrated faster regain of memory loss in amnesic mice with both PLGA and PBCA NPs when compared to RT solution. This indicates rapid and higher extent of transport of RT into the mice brain and thus shows the suitability of both NPs as potential carriers for providing sustained brain delivery of RT.

1. Introduction

Alzheimer's disease is the most common brain disease of adulthood. It has recently received a lot of attention, especially in areas related to novel treatments. It is a progressive and fatal disorder characterized by neuronal deterioration that results in loss of cognitive functions, such as memory, communication skills, judgments and reasoning [1]. Alzheimer's disease is 1.5 times more common than stroke or epilepsy and is as common as congestive heart failure [2]. It affects 15 million people worldwide. Moreover, Alzheimer's disease has a tremendous negative economic impact amounting to over $100 billion a year. Rivastigmine tartrate was approved by the US Food and Drug Administration for the treatment of AD, but its current therapy has many drawbacks that include restricted entry into brain due to its hydrophilicity, necessitating frequent dosing and cholinergic side effects.

Targeting of drugs to the brain is one of the most challenging issues for pharmaceutical research, as many hydrophilic drugs and neuropeptides are unable to cross the blood–brain barrier (BBB) [3]. The blood–brain barrier represents one of the hurdles for drugs including anti-Alzheimer, antibiotics, antineoplastic agents and a variety of neuroleptic drugs. Drug delivery to the brain requires advances in both drug delivery technologies and drug discovery. Drugs that are effective against diseases in the CNS and reach the brain via the blood compartment must pass the BBB. The management of brain-related diseases with presently available therapeutic system is very difficult, as insufficient amount of drug reaches the brain, due to highly lipophilic nature of the BBB. Many strategies have been developed to overcome this problem which includes chemical delivery systems, magnetic drug targeting or drug carrier systems such as antibodies, liposomes or nanoparticles [4–7]. Among these, polymeric NPs have recently attracted great attention as potential drug delivery systems. Due to their small size, NPs penetrate into even small capillaries and are taken up within cells, allowing an efficient drug accumulation at the targeted sites in the body. The use of biodegradable materials for NPs preparation allows sustained drug release at the targeted site over a period of days or even weeks after injection [8]. Drugs that have been successfully delivered into the brain using the car-

* Corresponding author. Address: TIFAC Centre of Relevance and Excellence, Centre of PG studies and Research, Pharmacy Department, The Maharaja Sayajirao University of Baroda, Donors Plaza, Fatehgunj, Vadodara, 390002, Gujarat, India. Tel.: +91 265 2434187; fax: +91 265 2418927.
E-mail address: dr_krutikasawant@rediffmail.com (K.K. Sawant).

0939-6411/$ - see front matter © 2010 Elsevier B.V. All rights reserved.
doi:10.1016/j.ejpb.2010.07.007

rier poly (butyl cyanoacrylate) include hexapeptide–dalargin [9], the dipeptide-kyotorphin [10], loperamide [11], tubocurarine [12], the NMDA receptor antagonist MRZ2/576 [13] and doxorubicin [14]. The delivery of drugs into the brain using NPs may open a new era for treating diseases such as Alzheimer's, multiple sclerosis and brain tumors.

Biodegradable NP can be successfully used for modulating the drug release profile by controlling the polymer degradation. One of the best known biodegradable carriers for controlled and sustained release is poly lactide-co-glycolide (PLGA) [15]. Features such as biocompatibility, prediction of biodegradation kinetics, ease of fabrication and regulatory approval has attracted its attention for a variety of biomedical applications [16,17].

Moreover, both hydrophilic and lipophilic drugs can be successfully encapsulated in the PLGA matrix [18]. PLGA has been used for delivery of drugs for both oral [19,20] and parenteral [21,22] routes. FDA has already approved some of the formulations using PLGA which are currently being marketed and others are at various stages of clinical trials [23]. PBCA is another biodegradable, biocompatible, bioabsorbable and bioadhesive polymer that has been widely investigated for controlled and targeted drug delivery. It has been reported that therapeutic agents, which normally cannot cross the BBB, can be transported across BBB by binding them to poly (butyl cyanoacrylate) NPs coated with Polysorbate 80 [24].

Rivastigmine tartrate (RT) is a reversible cholinesterase inhibitor used for the treatment of Alzheimer's disease. Rivastigmine has been shown to improve or maintain patients' performance in three major domains: cognitive function, global function and behavior. However, limitations with its oral therapy include restricted entry into brain due to its hydrophilicity, necessitating frequent dosing and cholinergic side effects like severe bradycardia, nausea, dyspepsia, vomiting and anorexia [25]. Hence, the present investigation was aimed at formulating nanoparticulate systems of RT that can improve brain targeting, provide sustained release, reduce dosing frequency and minimize side effects.

Traditionally, pharmaceutical formulations are developed by changing one variable at a time. The method is time-consuming, and it is difficult to evolve an ideal formulation using this classical technique since the combined effects of the independent variables are not considered. It is therefore important to understand the complexity of pharmaceutical formulations using established statistical tools such as factorial design [26]. Factorial designs, where all the factors are studied in all possible combinations, are considered to be the most efficient in estimating the influence of individual variables and their interactions using minimum experiments [27]. A prior knowledge and understanding of the process and the process variables under investigation are necessary for achieving a more realistic model. The independent variables are controllable, whereas responses are dependent. The contour plot gives a visual representation of the values of the response. This helps the process of optimization by providing an empirical model equation for the response as a function of the different variables, whereas three-dimensional response surface plots are very helpful in learning about both the main and interaction effects of the independent variables [28,29].

Hence, in the present study, RT-loaded nanoparticles of PLGA and PBCA were prepared and their formulation parameters were statistically optimized using 3^3 and 3^2 factorial designs, respectively. The optimized formulations were characterized for PS, PDE, TEM, and DSC. Further characterization was done for PBCA NPs by Fourier transform infrared (FTIR) spectroscopy and gel permeation chromatography (GPC). The formulations were evaluated for *in vitro* drug release, and the data obtained were fitted to Peppas model to understand the mechanism and kinetics of drug release. Pharmacodynamic study was performed in scopolamine-induced amnesic mice by Morris Water Maze Test.

2. Materials and methods

2.1. Materials

Rivastigmine tartrate (RT) was received as a gift sample from SPARC, Baroda, India. Poly (D, L Lactide-co-Glycolide) [Resomer 502 H] was received as a gift sample from Boehringer Ingelheim, Germany, and n-butyl cyanoacrylate (NBCA) monomer was received as a gift sample from Tong Shen Enterprise Co., Ltd., Taiwan and was used without further purification. Poloxamer 188 was purchased from Hi-media Labs, India. Pluronic F 127 was procured from Sigma Chemicals, Mumbai, India. Pluronic P85 was purchased from BASF, Germany. Polysorbate 80, disodium hydrogen phosphate, sodium tetraborate and sodium hydroxide were purchased from S.D. Finechem., Mumbai, India. Distilled water used in the study was filtered using 0.22-μm nylon filter (Nylon N66 membrane filters 47 mm, Rankem, India). All other chemicals and reagents used in this study were of analytical grade.

2.2. Preparation of PLGA and PBCA NPs

PLGA NPs were prepared by modified nanoprecipitation [30,31], and PBCA NPs were prepared by emulsion polymerization method [24,32]. In modified nanoprecipitation method, phosphate buffer with pH 9.0 was used as external medium instead of aqueous phase. In brief, 50 mg of PLGA and 7.5 mg RT were accurately weighed and dissolved in 5 ml acetone. This organic solution was added slowly to 10 ml solution of Pluronic F 127 (1%) in phosphate buffer (pH 9.0). The organic solvent was then allowed to evaporate for 4 h with continuous stirring on a magnetic stirrer (Remi). The NP suspension was then centrifuged at 25,000 rpm for 1 h at 4 °C using high-speed centrifuge (Sigma). Supernatant was analyzed for free drug content, and sediment constituting NPs was freeze-dried using trehalose dihydrate as cryoprotectant (Heto dry winner, Denmark).

PBCA NPs were prepared by in situ anionic emulsion polymerization method. Poloxamer 188 (1%) was dissolved in 20 ml 0.01 N HCl, while RT (7.5 mg) was dissolved in 1% of nBCA. Then the monomer solution containing drug was slowly added to the aqueous phase under stirring on magnetic stirrer, and the monomer was allowed to polymerize. After 4 h, the NPs suspension was neutralized to pH 7.0 using 0.1 N NaOH, and stirring was continued for 1 h to complete the polymerization. The dispersion was incubated in 1% Polysorbate 80 solution for 30 min and centrifuged at 25,000 rpm for 1 h. Then, supernatant was analyzed for free drug content, and sediment comprising of the NPs was freeze-dried using trehalose dihydrate as cryoprotectant [33].

2.3. Factorial design and optimization

Based on the results obtained in preliminary experiments, surfactant concentration (X_1), polymer concentration (X_2) and volume of internal phase (X_3) were found to be the major variables affecting PS and PDE for PLGA NPs, while those for PBCA NPs were surfactant concentration (X_1) and monomer concentration (X_2). Hence, 3^3 factorial design was applied for PLGA NPs and 3^2 factorial design was applied for PBCA NPs to find the optimized condition for minimum PS and highest PDE. The formulation parameters for factorial design of PLGA and PBCA NPs are shown in Table 1 and Table 2 respectively. In developing the regression equation, the test factors were coded according to

$$x_i = \left(X_i - X_i^X\right)/\Delta X_i \quad (1)$$

where x_i is the coded value of the ith independent variable, X_i is the natural value of the ith independent variable, X_i^X is the natural value of the ith independent variable at the center point and ΔX_i is the step change value. Multiple regression according to quadratic model was carried out using

$$Y = b_0 + \sum_i b_i X_i + \sum_i \sum_y b_{ij} X_i X_j + \sum b_{ii} X_i^2 \quad (2)$$

where Y is the measured response, b_0 is the intercept term, b_i, b_{ij}, and b_{ii} are, respectively, the measures of the variables X_i, X_iX_j, and X_i^2. The variable X_iX_j represents the first-order interactions between X_i and X_j ($i < j$). [34,35].

The multiple regression was applied using Microsoft excel in order to deduce the factors having significant effect on the formulation properties, and the best fitting mathematical model was selected [36]. Three-dimensional response surface plots and two-dimensional contour plots resulting from equations were obtained by the NCSS software.

3. Characterization

3.1. Determination of particle size (PS), Zeta (ζ) potential and percentage drug entrapment (PDE)

The PS and ζ-potential of the RT-loaded PLGA and PBCA NPs were characterized by Photon Correlation Spectroscopy using Particle Size Analyzer (Malvern Zeta Sizer Nano ZS, UK). The amount of drug entrapped in NPs was estimated by UV spectrophotometer (Shimadzu 1700, Japan). The NPs suspension was subjected to centrifugation at 25,000 rpm for 1 h at 4 °C. Definite amount of sedimented NPs was dissolved in acetonitrile and diluted appropriately, and absorbance was recorded at 264 nm. All tests were performed in triplicate.

3.2. Fourier transform infrared (FTIR) spectroscopy

FTIR studies were carried out to confirm complete polymerization of nBCA monomer into PBCA. FTIR spectra of nBCA monomer and RT-loaded PBCA NPs were recorded on Shimadzu Fourier Transform Infrared Spectrophotometer (Shimadzu 8400S, Japan). Test samples were mixed with KBr, pressed into a disk and scanned from 400 to 4000 cm^{-1}.

3.3. Molecular weight determination

Gel permeation chromatography (GPC) was carried out to determine the molecular weight of the formed polymer [37,38]. The molecular weight of BCA polymer was determined by GPC equipped with a Waters 510 pump, 50, 10–3, and 10–4 °A Phenogel columns serially set (Phenomenex, USA) and a Waters 410 differential refractometer. The mobile phase was tetrahydrofuran (THF) at a flow rate of 1.0 ml/min. Fifty microliters of a 2% polymer solution in THF was injected into the system, and size exclusion chromatogram was recorded.

3.4. Differential scanning calorimetry (DSC)

The physical state of RT entrapped in the NPs was characterized by Differential Scanning Calorimetry (DSC-60, Shimadzu, Japan). Each sample was sealed in standard aluminum pans with lids and purged with air at a flow rate of 40 ml/min. A temperature ramp speed was set at 20 °C/min, and the heat flow was recorded in the range of 30–300 °C under inert nitrogen atmosphere. Thermograms were taken for RT, PLGA, RT-loaded PLGA NPs and RT-loaded PBCA NPs.

3.5. Transmission electron microscopy (TEM)

TEM analysis of the prepared formulations was carried out to understand the morphology of nanoparticles. A drop of NPs suspension containing 0.01% of phosphotungstic acid was placed on a carbon film coated on a copper grid for TEM. TEM studies were performed at 80 kV using PHILIPS TECHNAI-20, Japan. The copper grid was fixed into sample holder and placed in vacuum chamber of the transmission electron microscope and observed under low vacuum, and TEM images were recorded.

3.6. In vitro release studies

A modified dialysis method [39,40] was used to evaluate the *in vitro* release of RT-loaded PLGA and PBCA NPs. Two milliliters of nanoparticle suspension (corresponding to 1.5 mg of RT) was placed in a dialysis bag (cellophane membrane, molecular weight cut off 10,000–12,000, Hi-Media, India), which was tied and placed into 20 ml of phosphate buffer (0.1 M, pH 7.4), maintained at 37 °C with continuous magnetic stirring. At selected time intervals, aliquots were withdrawn from the release medium and replaced with the same amount of phosphate buffer. The sample was assayed spectrophotometrically for RT at 264 nm. The data obtained from *in vitro* drug release were fitted to Peppas model [41] to understand the mechanism of drug release from the NPs. The studies were performed in triplicate.

3.7. Pharmacodynamic study

To evaluate the influence of developed NPs formulation on learning and memory capacities, Morris Water Maze Test was performed in scopolamine-induced amnesia model in mice [42,43]. Mice were evaluated once daily (three cycles) for two water maze test for four consecutive days with an inter-trial interval of 2 min. In the first test, mice were placed on the platform for 20 s and then placed in the water. Escape latency (indicative of learning and intact reference memory) was measured. After 20 s on the platform, the animals were placed back in the water (in previous position) and allowed to search for platform (retained in previous position). Escape latency (indicative of Short-term Working Memory, i.e. second test) was recorded. The platform location and the animal's starting point were changed every day. Amnesia was induced by intraperitoneal (i.p.) injection of scopolamine hydrochloride (0.4 mg/kg of body weight (BW)) in 0.9% saline (NS) 30 min prior to testing. Mice were divided into two groups: saline treated (i.p.) and scopolamine-treated (i.p. 0.4 mg/kg). In both groups, animals ($n = 4$) were administered different formulations (i.e., RT solution {RS}, PLGA NPs {RNP}, PBCA NPs {RNPB} – 1.5 mg/kg) and evaluated once daily (three cycles) for two water maze test for four consecutive days as described above. The formulations were injected intravenously (i.v.) through tail vein of mice. This protocol has been approved by Institutional Animal Ethical Committee (IAEC).

3.8. Statistical analysis

All data are reported as mean ± SEM, and the difference between the groups was tested using Student's '*t*' test at the level

Table 1
Coded values of the formulation parameters for PLGA NPs.

Coded values	Actual values		
	X_1 (% w/v)	X_2 (mg)	X_3 (ml)
−1	0.5	25	2.5
0	1	37.5	3.5
1	1.5	50	5

X_1–Surfactant concentration, X_3–Volume of internal phase, X_2–Polymer concentration

Table 2
Coded values of the formulation parameters of PBCA NPs.

Coded values	Actual values	
	X_1 (% w/v)	X_2 (μl)
−1	0.5	100
0	1	200
1	1.5	300

X_1–Surfactant concentration, X_2–Monomer concentration

of $p < 0.05$. More than two groups were compared using ANOVA, and differences greater at $p < 0.05$ were considered significant.

4. Results and discussion

4.1. Preparation and optimization by factorial design

Using 3^3 factorial design as shown in Table 3, 27 batches of PLGA NPs were prepared varying three independent variables, surfactant concentration (X_1), polymer concentration (X_2) and volume of organic phase (X_3). The PS and PDE responses are recorded in Table 3. The results of the regression output and response of full model and reduced model of PLGA NPs are presented (Table 3). Minimum PS and maximum PDE achieved were 135.6 ± 4.2 nm and 74.46 ± 0.76%, respectively, at 0 level of X_1 (1% w/v), +1 level of X_2 (50 mg) and +1 level of X_3 (5 ml). The equations for full and reduced model are given in Eqs. (3)–(6).

Full model for PLGA NPs

$$Y1(PS) = 121.470 + 14.05X_1 + 16.95X_2 - 10.80X_3 - 0.62778X_1^2 + 2.0X_2^2 + 0.155X_3^2 + 1.025X1X2 - 1.825X_2X_3 - 1.210X_1X_3 + 0.4X_1X_2X_3 \quad (3)$$

$$Y2(PDE) = 72.287 + 0.945X_1 + 2.09X_2 - 1.632X_3 - 0.409X_1^2 + 0.6388X_2^2 - 0.4261X_3^2 + 0.3691X_1X_2 + 0.518X_2X_3 + 0.3084X_1X_3 + 0.2812X_1X_2X_3 \quad (4)$$

Reduced model for PLGA NPs

$$Y1(PS_{red}) = 121.470 + 14.05X_1 + 16.95X_2 - 10.667X_3 \quad (5)$$

$$Y2(PDE_{red}) = 71.73 + 0.945X_1 + 2.09X_2 - 1.6672X_3 + 0.6388X_2^2 + 0.3691X_1X_2 + 0.5183X_2X_3 \quad (6)$$

The positive sign for the coefficient of X_1 and X_2 in Eqs. (5) and (6) showed that PS and PDE can be increased by an increase in X_1 and X_2. However, negative sign for the coefficient X_3 showed that PS and PDE increased by decrease in X_3.

The results of ANOVA of the second-order polynomial equation are given in Tables 4a and 4b for PS and PDE, respectively. *F*-Statistic of the results of ANOVA of full and reduced model confirmed omission of non-significant terms of Eqs. (3) and (4). Since the calculated *F* value (0.5178) was less than the tabled *F* value (2.66) ($\alpha = 0.05$, $V_1 = 7$ and $V_2 = 16$) for PS, it was concluded that the neglected terms do not significantly contribute in the prediction; however, calculated *F* value (3.4265) was more than the tabled *F* value (3.01) ($\alpha = 0.05$, $V_1 = 4$ and $V_2 = 16$) for PDE, indicating that the neglected terms could also significantly contribute in the prediction [44]. The goodness of fit of the model was checked by the

Table 4a
Analysis of variance (ANOVA) of PS for full and reduced models of PLGA NP[a].

	DF	SS	MS	*F*	*R*	R^2	Adj. R^2
Regression							
FM	10	10867.51	1086.751	41.545	0.9812	0.9629	0.9397
RM	3	10772.59	3590.897	160.886	0.9769	0.9545	0.9485
Error							
FM	16	418.529(E1)	26.158				
RM	23	513.348(E2)	22.319				

SSE2–SSE1 = 513.348– 418.529 = 94.81936.
No. of parameters omitted = 7 MS of error (full model) = 26.158.
F calculated = (SSE2–SSE1/no. of parameters omitted)/MS of error (full model) = (94.81936/7)/26.158 = 0.517837.
Tabled *F* value = 2.66 ($\alpha = 0.05$, $V_1 = 7$, and $V_2 = 16$).
[a] Where DF indicates degrees of freedom; SS sum of square; MS mean sum of square and *F* is Fischer's ratio.

Table 3
Full factorial (3^3) design layout for PLGA NPs.

Batch no.	X_1	X_2	X_3	X_1^2	X_2^2	X_3^2	X_1X_2	X_1X_3	X_2X_3	$X_1X_2X_3$	PS[a] (±SEM)	PDE[a] (±SEM)
1	−1	−1	−1	1	1	1	1	1	1	−1	100.4 (6.8)	71.53(1.59)
2	−1	−1	0	1	1	0	1	0	0	0	91.6 (8.3)	69.86 (2.33)
3	−1	−1	1	1	1	1	1	−1	−1	1	85.5 (3.7)	67.39 (0.46)
4	−1	0	−1	1	0	1	0	1	0	0	121.7 (10.9)	72.65 (1.99)
5	−1	0	0	1	0	0	0	0	0	0	113.8 (3.7)	71.42 (0.91)
6	−1	0	1	1	0	1	0	−1	0	0	101.4 (12.5)	68.21 (1.63)
7	−1	1	−1	1	1	1	−1	1	−1	1	132 (5.4)	74.19 (0.56)
8	−1	1	0	1	1	0	−1	0	0	0	119.5 (2.3)	73.76 (0.77)
9	−1	1	1	1	1	1	−1	−1	1	−1	108.2 (15.6)	70.66 (0.11)
10	0	−1	−1	0	1	1	0	0	1	0	111.2 (7.6)	72.27 (0.48)
11	0	−1	0	0	1	0	0	0	0	0	103.5 (10.5)	71.64 (0.89)
12	0	−1	1	0	1	1	0	0	−1	0	94.9 (6.3)	68.34 (2.93)
13	0	0	−1	0	0	1	0	0	0	0	129.7 (7.5)	73.23 (3.00)
14	0	0	0	0	0	0	0	0	0	0	118.6 (1.3)	72.19 (1.32)
15	0	0	1	0	0	1	0	0	0	0	110.3 (16.3)	69.61 (1.56)
16	0	1	−1	0	1	1	0	0	−1	0	159.2 (16.0)	75.64 (1.03)
17	0	1	0	0	1	0	0	0	0	0	143.2 (9.6)	75.08 (2.34)
18	**0**	**1**	**1**	**0**	**1**	**1**	**0**	**0**	**1**	**0**	**135.6 (4.2)**	**74.46 (0.76)**
19	1	−1	−1	1	1	1	−1	−1	1	1	132.5 (6.9)	73.12 (0.84)
20	1	−1	0	1	1	0	−1	0	0	0	125.7 (2.6)	70.15 (1.76)
21	1	−1	1	1	1	1	−1	1	−1	−1	110.6 (12.0)	68.81 (4.23)
22	1	0	−1	1	0	1	0	0	0	0	143.8 (6.3)	74.26 (0.33)
23	1	0	0	1	0	0	0	0	0	0	131.5 (8.0)	73.15 (2.99)
24	1	0	1	1	0	1	0	0	0	0	119.6 (13.7)	70.85 (4.85)
25	1	1	−1	1	1	1	1	−1	−1	−1	168.4 (8.1)	76.24 (1.09)
26	1	1	0	1	1	0	1	0	0	0	154.1 (6.4)	75.31 (1.54)
27	1	1	1	1	1	1	1	1	1	1	140.8 (14.2)	74.79 (3.22)

[a] $n = 3$.

Table 4b
Analysis of variance (ANOVA) of PDE for full and reduced models of PLGA NP [a].

	DF	SS	MS	F	R	R^2	Adj. R^2
Regression							
FM	10	155.7002	15.57	58.336	0.9865	0.9733	0.9566
RM	6	152.0421	25.3403	63.921	0.9749	0.9504	0.9355
Error							
FM	16	4.2704 (E1)	0.2669				
RM	20	7.9285 (E2)	0.3964				

SSE2–SSE1 = 7.9285–4.2704 = 3.65813.
No. of parameters omitted = 4 MS of error (full model) = 0.2669.
F calculated = (3.65813/4)/0.2669 = 3.426485.
Tabled *F* value = 3.01 ($\alpha = 0.05$, $V_1 = 4$, and $V_2 = 16$).
[a] Where DF indicates degrees of freedom; SS sum of square; MS mean sum of square and *F* is Fischer's ratio.

determination coefficient (R^2). In this case, the values of the determination coefficients (R^2) and adjusted determination coefficients (adj R^2) were very high (>90%), which indicates a high significance of the model. All the above considerations indicate an adequacy of the regression model [45,46].

Nine batches of PBCA NPs were prepared using 3^2 factorial design, varying two independent variables, surfactant concentration (X_1) and monomer concentration (X_2). The PS and PDE were taken as dependent variables, and the results are recorded in Table 5. Minimum PS and maximum PDE achieved were 146.8 ± 2.6 nm and 57.32 ± 0.91%, respectively, at 0 level of X_1 and X_2.

The regression equations for the models (full and reduced) *Y*1 and *Y*2 are shown in Eqs. (7)–(10).

$$Y1(PS) = 145.44 - 29.16X_1 + 10.83X_2 - 9.16X_1^2 - 0.16X_2^2 + 0.25X_1X_2 \quad (7)$$

$$Y2(PDE) = 57.36 - 2.16X_1 + 3.61X_2 - 0.34X_1^2 + 0.26X_2^2 + 0.115X_1X_2 \quad (8)$$

$$Y1(PS_{red}) = 145.44 - 29.16X_1 + 10.83X_2 - 9.16X_1^2 \quad (9)$$

$$Y2(PDE_{red}) = 57.36 - 2.16X_1 + 3.61X_2 \quad (10)$$

The results of ANOVA of the second-order polynomial equation are given in Tables 6a and 6b for PS and PDE, respectively. *F*-Statistic of the results of ANOVA of full model and reduced model confirmed omission of insignificant terms of Eqs. (7) and (8). Since the calculated *F* values for both PS and PDE were less than the tabled *F* values [44], it was concluded that the neglected terms do not significantly contribute in the prediction of PS and PDE. When the coefficients of the two independent variables in Eqs. (9) and (10) were compared, the value for the variable X_1 ($b_1 = -29.16$) was found to be maximum for PS and hence, it was considered to be a major contributing variable for PS. In case of PDE, the value for the variable X_2 ($b_2 = 3.61$) was found to be maximum and hence, it was considered to be a major contributing variable for improving

Table 5
Full factorial (3^2) design layout for PBCA NPs.

Batch No.	X_1	X_2	X_1^2	X_2^2	X_1X_2	PS[a] (±SEM)	PDE[a] (±SEM)
1	−1	−1	1	1	1	156.7 (5.8)	56.23 (1.59)
2	−1	0	1	0	0	166.6 (6.3)	59.08 (2.33)
3	−1	1	1	1	−1	174.5 (3.7)	62.78 (0.46)
4	0	−1	0	1	0	131.0 (11.9)	53.57 (1.99)
5	0	0	0	0	0	146.8 (2.7)	57.32 (0.91)
6	0	1	0	1	0	159.4 (12.5)	61.72 (1.63)
7	1	−1	1	1	−1	98.2 (7.4)	51.54 (0.56)
8	1	0	1	0	0	106.5 (2.3)	55.01 (0.77)
9	1	1	1	1	1	117.2 (5.6)	58.55 (0.11)

[a] $n = 3$.

Table 6a
Analysis of variance (ANOVA) of PS for full and reduced models of PBCA NP [*].

	DF	SS	MS	*F*	*R*	R^2	Adj. R^2
Regression							
FM	5	5976.694	1195.34	109.13	0.9976	0.9945	0.9854
RM	3	5976.389	1992.13	300.321	0.9972	0.9944	0.9911
Error							
FM	3	32.86 (E1)	10.95				
RM	5	33.16 (E2)	6.63				

SSE2–SSE1 = 33.16 – 32.86 = 0.3055.
No. of parameters omitted = 2.
MS of error (full model) = 10.95.
F calculated = (0.3055/2)/10.95 = 0.01394.
Tabled *F* value = 9.55 ($\alpha = 0.05$, $V_1 = 2$, and $V_2 = 3$).
[*] Where DF indicates degrees of freedom; SS sum of square; MS mean sum of square and *F* is Fischer's ratio.

Table 6b
Analysis of variance (ANOVA) of PDE for full and reduced models of PBCA NP[*].

	DF	SS	MS	*F*	*R*	R^2	Adj. R^2
Regression							
FM	5	107.096	21.42	94.448	0.9968	0.9937	0.9832
RM	2	106.677	53.34	291.170	0.9949	0.9898	0.9864
Error							
FM	3	0.680 (E1)	0.2268				
RM	6	1.099 (E2)	0.1831				

SSE2–SSE1 = 1.099 – 0.680 = 0.4187.
No. of parameters omitted = 3.
MS of error (full model) = 0.2268.
F calculated = (0.4187/3)/0.2268 = 0.61553.
Tabled *F* value = 19.2 ($\alpha = 0.05$, $V_1 = 3$ and $V_2 = 2$).
[*] Where DF indicates degrees of freedom; SS sum of square; MS mean sum of square and *F* is Fischer's ratio.

entrapment efficiency of PBCA NPs. The Fisher *F* test with a very low probability value ($P_{model} > F = 0.000001$) demonstrated a very high significance for the regression model. The goodness of fit of the model was checked by the determination coefficient (R^2). In this case, the values of the determination coefficients indicated that over 98% of the total variations are explained by the model. The values of adjusted determination coefficients (adj R^2) are also very high (>98%) which indicates a high significance of the model. All the above considerations indicate an excellent adequacy of the regression model [45,46].

4.1.1. Contour plots

Fig. 1a–c is the contour plot for PLGA NPs for prefixed PS values which were found to be non-linear with curved segment signifying non-linear relationship between variables X_2 and X_3. It was observed that minimum PS (85.5 nm) could be obtained with X_2 between 25 mg and 29.41 mg and X_3 between 4.79 ml and 5 ml. Fig. 1d–f shows the contour plots for prefixed PDE values which were also found to be non-linear and having curved segment indicating non-linear relationship between variables X_2 and X_3. It was determined from the contour that maximum PDE (74.19%) could be obtained with X_2 between 45.58 mg and 50 mg and X_3 between 2.5 ml and 2.94 ml.

In case of PBCA NPs, two-dimensional contour plots were found to be non-linear which indicate non-linear relationship between X_1 and X_2 variables. From the contour, it was observed that higher amount of surfactant and lower amount of monomer are necessary for minimum PS (Fig. 2a). Similarly, the contour plot for PDE was also non-linear showed that lower amount of surfactant and higher amount of monomer are necessary for maximum PDE (Fig. 2b).

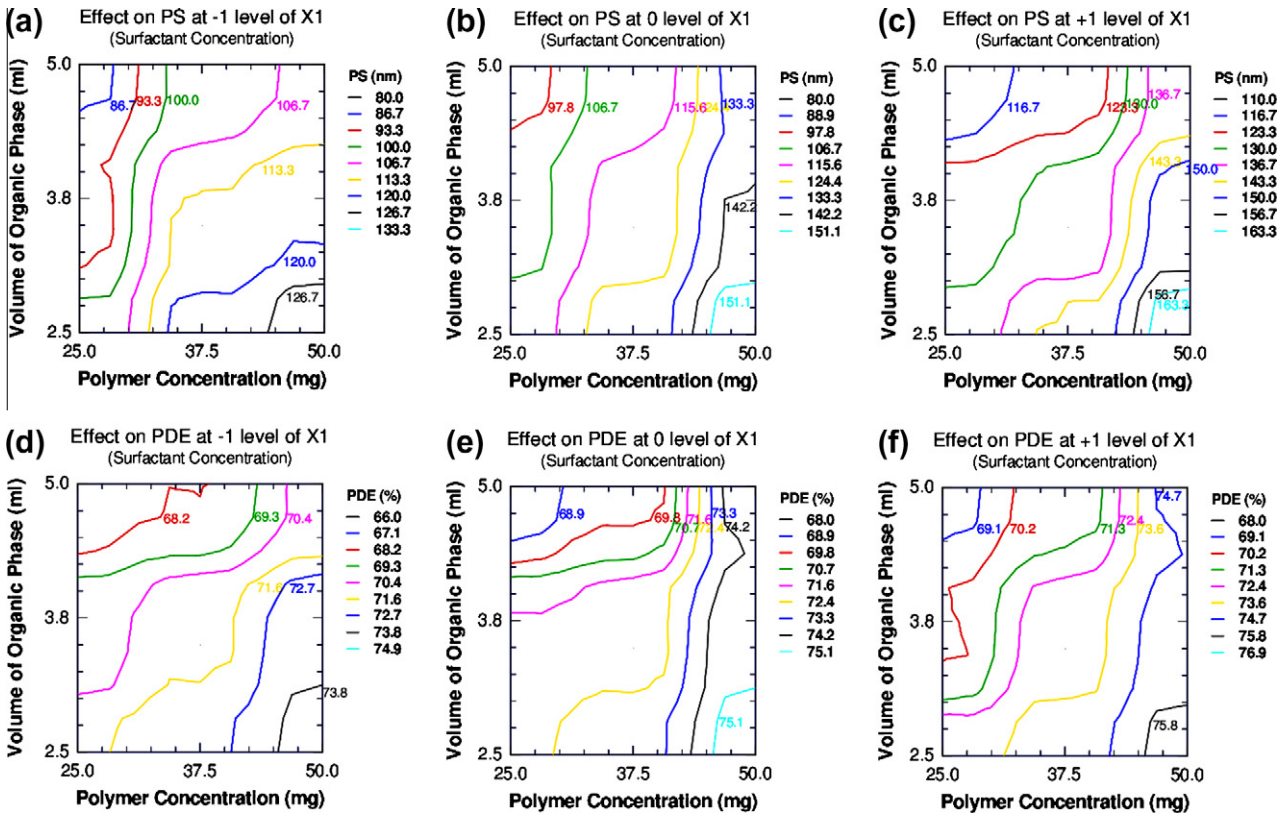

Fig. 1. Contour plots for PLGA NPs: (a) effect on PS at −1 level of surfactant concentration (X_1), (b) effect on PS at 0 level of X_1, (C) Effect on PS at +1 level of X_1, (d) effect on PDE at −1 level of X_1, (e) effect on PDE at 0 level of X_1, and (f) effect on PDE at +1 level of X_1. (For interpretation of the references to colour in this figure legend, the reader is referred to the web version of this article.)

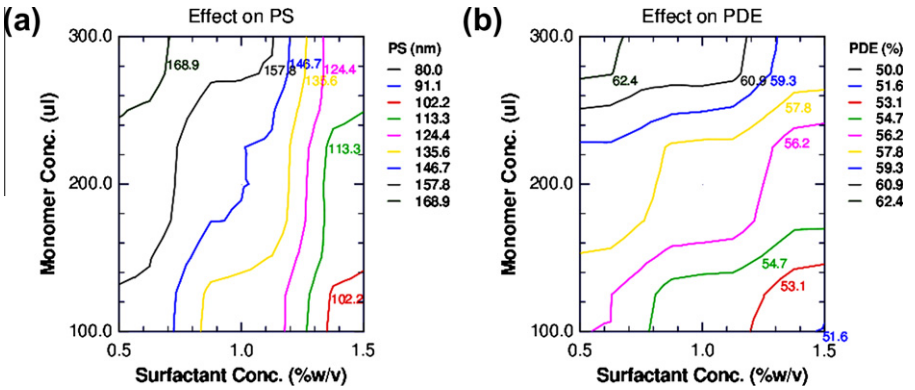

Fig. 2. Contour plots for PBCA NPs: (a) effect on PS of PBCA NPs and (b) effect on PDE of PBCA NPs. (For interpretation of the references to colour in this figure legend, the reader is referred to the web version of this article.)

4.1.2. Response surface plots

Three-dimensional response surface plots generated by the NCSS software are presented in Figs. 3 and 4, for PLGA NPs and PBCA NPs, respectively. Fig. 3a–c depicts response surface plots for PS of PLGA NPs which show an increase in PS with increase in the polymer concentration and decrease in volume of organic phase. Fig. 3d–f depict response surface plots for PDE at constant level of the factor X_1 which indicate an increase in PDE with increase in the polymer concentration and decrease in volume of organic phase.

Fig. 4a and b are the response surface plots for PBCA NPs which show decrease in PS with increase in surfactant concentration and decrease in monomer concentration while increase in PDE was observed with increase in monomer concentration and decrease in surfactant concentration.

4.2. Characterization

4.2.1. Particle size (PS), zeta (ζ) potential and percentage drug entrapment (PDE)

The PLGA and PBCA NPs formed were uniform, discrete and < 200 nm in size. Smaller particles have a larger free surface, which can lead to a faster release of a drug incorporated [47]. A possible endocytosis of the particles, for example, is size depen-

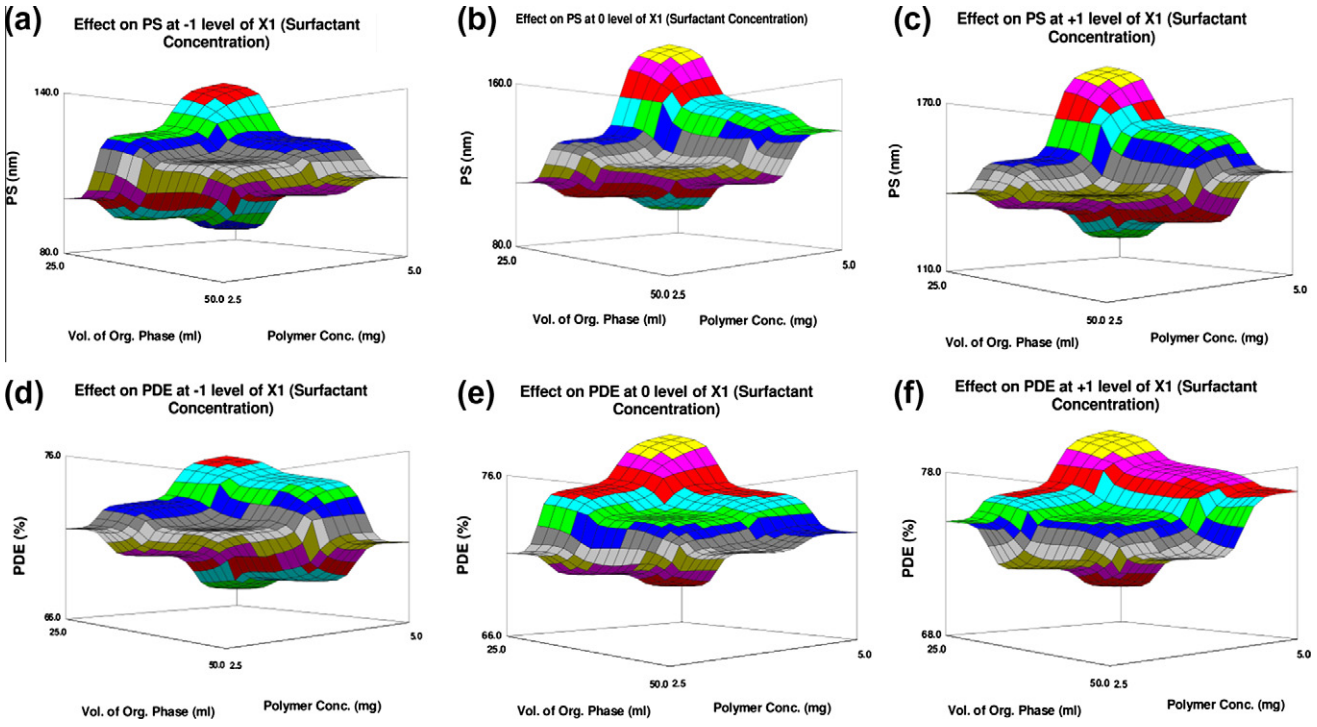

Fig. 3. Response surface plots for PLGA NPs: (a) effect on PS at −1 level of surfactant concentration (X_1), (b) effect on PS at 0 level of X_1, (c) effect on PS at +1 level of X_1, (d) effect on PDE at −1 level of X_1, (e) effect on PDE at 0 level of X_1, and (f) effect on PDE at +1 level of X_1. (For interpretation of the references to colour in this figure legend, the reader is referred to the web version of this article.)

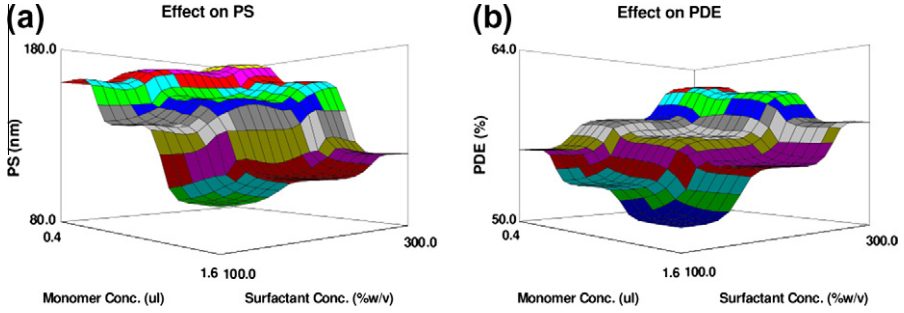

Fig. 4. Response surface plots PBCA NPs: (a) effect on PS of PBCA NPs and (b) effect on PDE of PBCA NPs. (For interpretation of the references to colour in this figure legend, the reader is referred to the web version of this article.)

dent [48]. NPs of PLGA had an average particle size of 135.6 ± 4.2 nm and for PBCA it was 146.8 ± 2.7 nm. The ζ-potential of PLGA NPs was found to be −23.7 ± 1.18 mV, whereas ζ-potential of PBA NPs was found to be −13.9 ± 0.58 mV. High negative charges of ζ-potential indicate that the electrostatic repulsion between particles with the same electrical charge will prevent the aggregation of the spheres and could stabilize particle suspensions [49]. A high entrapment efficiency of 74.46 ± 0.7% for PLGA NPs was obtained. PLGA NPs have been reported to give high entrapment efficiencies for water-insoluble drugs [21], but present investigation reveals that modified nanoprecipitation method can lead to NPs with high entrapment with water-soluble drug such as RT [50]. This would be beneficial in incorporating the required dose in minimum volume, facilitating parenteral administration of the NPs formulation. PDE for PBCA NPs was 57.32 ± 0.9% because of less solubility of RT in polymerization medium [51].

4.2.2. Differential scanning calorimetry (DSC)

DSC thermograms of RT, polymer (PLGA), dummy PBCA NPs and RT-loaded freeze-dried PLGA and PBCA NPs are shown in Fig. 5. Drug-loaded NPs showed endothermic peak at 48.20 °C and 192.9 °C attributed to PLGA and PBCA, respectively. However, the peak at 126.13 °C exhibited by RT was not visible in both the RT-loaded NPs, indicating that RT was encapsulated by the polymers in the NPs.

4.2.3. Transmission electron microscopy (TEM)

The morphological characteristics of the NPs were observed using TEM. The images of PLGA and PBCA NP are shown in

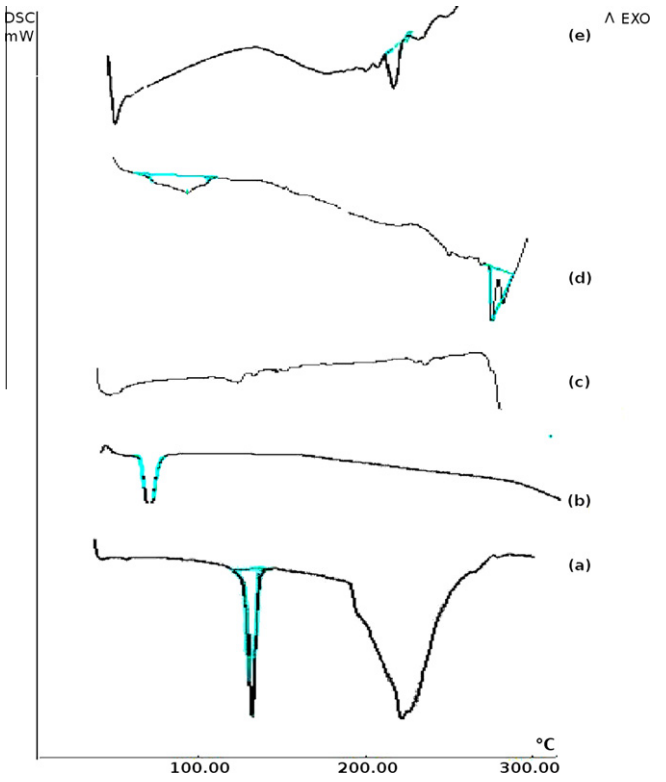

Fig. 5. DSC thermograms (a) RT, (b) polymer (PLGA), (c) dummy PBCA NPs, (d) RT-loaded freeze-dried PLGA, and (e) RT-loaded freeze-dried PBCA NPs. (For interpretation of the references to colour in this figure legend, the reader is referred to the web version of this article.)

Fig. 6a and b, respectively. The images reveal that both NPs were spherical in shape, but PLGA NPs were non-aggregated, while PBCA NPs were slightly aggregated, probably due to the inherent adhesive property of PBCA (cyanoacrylate MSDS).

4.2.4. Fourier transform infrared (FTIR) spectroscopy

The Fourier transform infrared (FTIR) spectra of the nBCA monomer and PBCA NPs are shown in Fig. 7a and b, respectively. Fig. 7a shows C–H (str) at 2957 cm^{-1} and C–H (def) at 1461 cm^{-1}. The characteristic C≡N (str) of the nBCA was observed at 2200 cm^{-1}. A prominent peak at 1750 cm^{-1} corresponding to C=O (str) and C–O (str) was observed at 1259 cm^{-1}. Fig. 7b shows all the peaks of nBCA monomer along with the characteristic peak of –OH stretching at 3465 cm^{-1} related to PBCA, which indicates polymerization of nBCA monomer [52].

4.2.5. Molecular weight determination

From the results of gel permeation chromatography (Fig. 8), the molecular weight of PBCA NPs was found to be 4216 Da which is in accordance with previously reported value [53].

4.2.6. In vitro drug release study

The release profile of the drug-loaded PLGA NPs and PBCA NPs is shown in Fig. 9. Drug release studies of drug-loaded NPs showed biphasic release profile for both PLGA and PBCA NPs. The initial fast release rate may be due to smaller particle size of NPs which is associated with smaller diffusion path, so drug accessible to the solid/dissolution medium interface can diffuse easily to the surface [54]. Thereafter, the release rate decreased that reflects the release of drug entrapped in the polymer. The release rate in the second phase is assumed to be controlled by diffusion rate of drug across the polymer matrix [55]. Huang and Lee reported that for PBCA, the longer hydrophobic alkyl side chains would shield effectively against the hydroxyl ions to attack the ester groups of polymer and therefore decrease the hydrolysis rate [56], which might also be responsible for the slower release from PBCA NPs. In case of PLGA NPs, the release rate is dependent upon the molecular weight and lactide content of the polymer. The release rate reduces as the molecular weight and lactide content of the polymer increase. The drug release rate of PLGA NPs is slower than PBCA NPs, which may be due to the higher molecular weight of PLGA (12,000 Da, as per MSDS) than PBCA (4216 Da, as determined by GPC), which may increase the lag time before the commencement of the polymer degradation controlled phase [57].

When the data obtained from *in vitro* release studies were fitted to Korsmeyer–Peppas model, it showed n value (diffusion exponent) <0.5, suggesting that the release pattern followed first-order, Fickian diffusion kinetics/anomalous transport for both PLGA and PBCA NPs [57]. The R^2 values for PLGA and PBCA for Korsmeyer–Peppas model are 0.949 and 0.960 indicating a good model fit.

4.2.7. Pharmacodynamic study (Morris Water Maze Test)

The effects of RT formulations after intravenous administration on the escape latency achieved in the Morris Water Maze Test in saline and scopolamine-treated mice are shown graphically in Fig. 10a and b, respectively. Saline-treated mice rapidly learnt the location of the platform as indicated by gradual decrease in es-

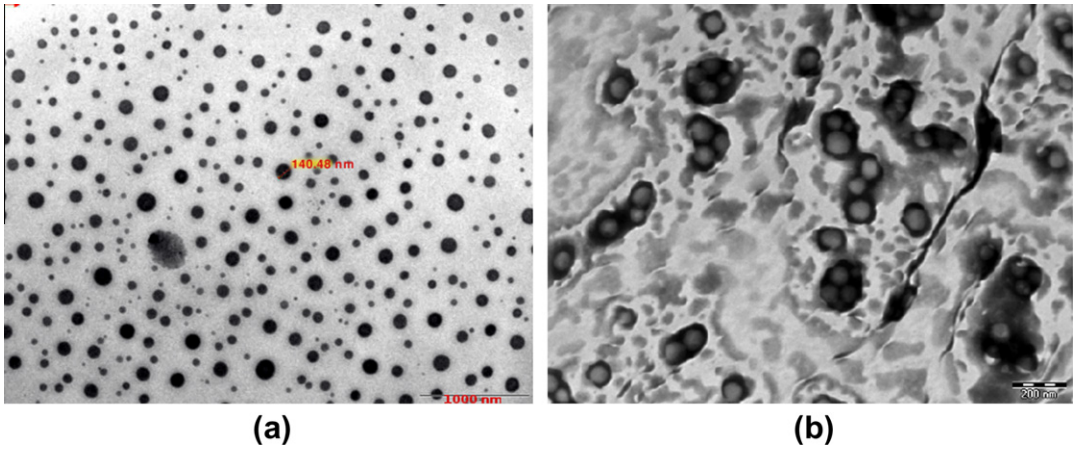

Fig. 6. TEM image (a) PLGA NPs and (b) PBCA NPs. (For interpretation of the references to colour in this figure legend, the reader is referred to the web version of this article.)

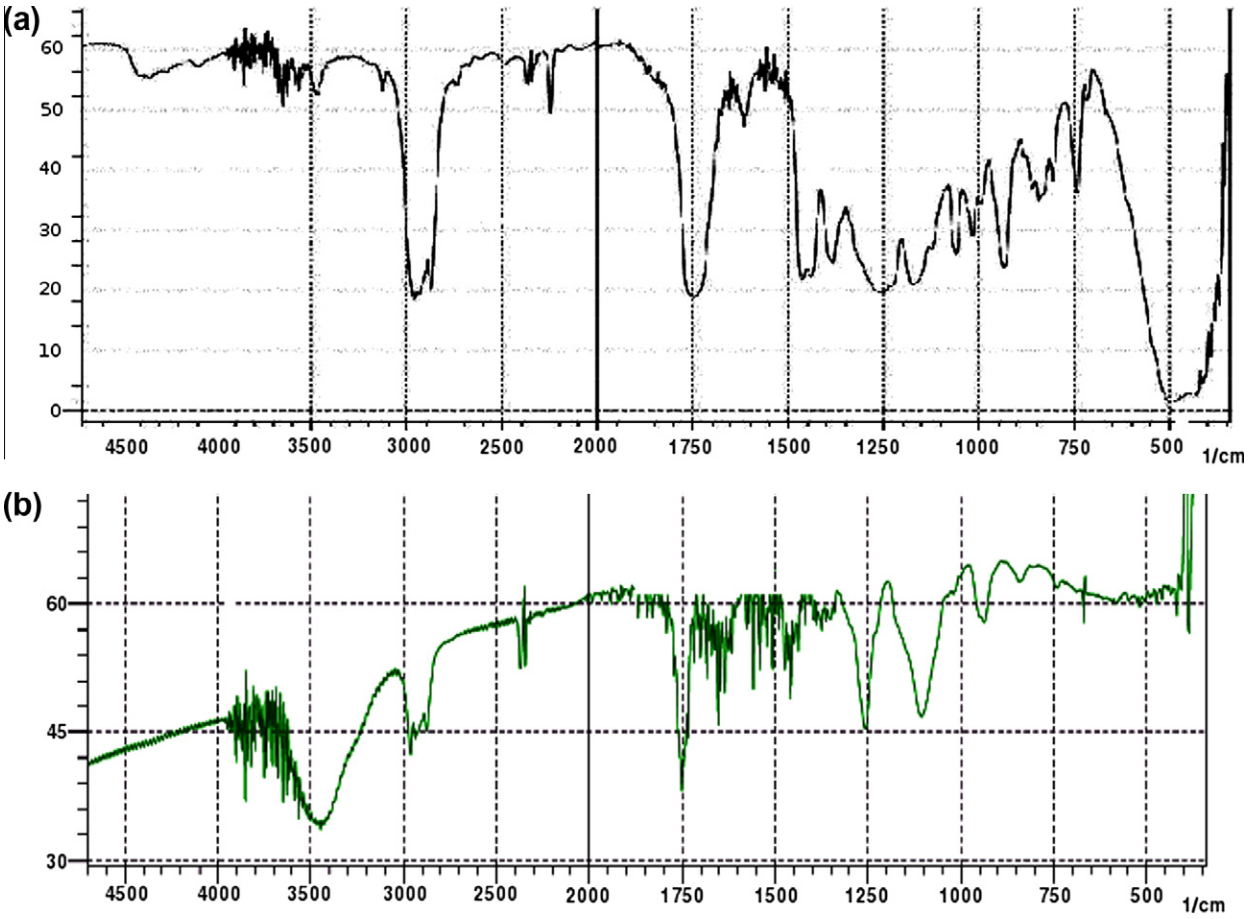

Fig. 7. FTIR spectrum (a) BCA monomer and (b) PBCA NPs. (For interpretation of the references to colour in this figure legend, the reader is referred to the web version of this article.)

cape latency. Minimum escape latency was achieved on day 3 in both Tests 1 and 2 and thereafter no significant decrease in escape latency was observed (Fig. 10a and b) In the scopolamine-treated mice, a characteristic swimming behavior consisting of circling around the pool was observed, indicating loss of memory and the latency period in learning and intact reference memory (Test 1) and short-term working memory (Test 2) remained unchanged throughout 4 days of testing period (Fig. 10a and b). Administration of RT formulations in saline-treated mice did not result in any noticeable improvement in learning and memory capacities, while administration of RT formulations in scopolamine-treated mice antagonized the scopolamine-induced amnesia as evidenced by significant decrease in escape latency in both tests (Fig. 10c and d). These results indicated an increase in learning and memory capacities associated with RT. Following intravenous injection of RT-loaded PLGA NPs (RNP), mice learnt to reach the platform within 3 days and exhibited behavioral pattern identical to saline-treated control mice, while similar behavior was observed at the end of 4 days in case of RT-loaded PBCA NPs (RNPB). In case of intravenous injection RT solution (RS), a decrease in the escape latency and improvement in learning and memory were observed. But, it

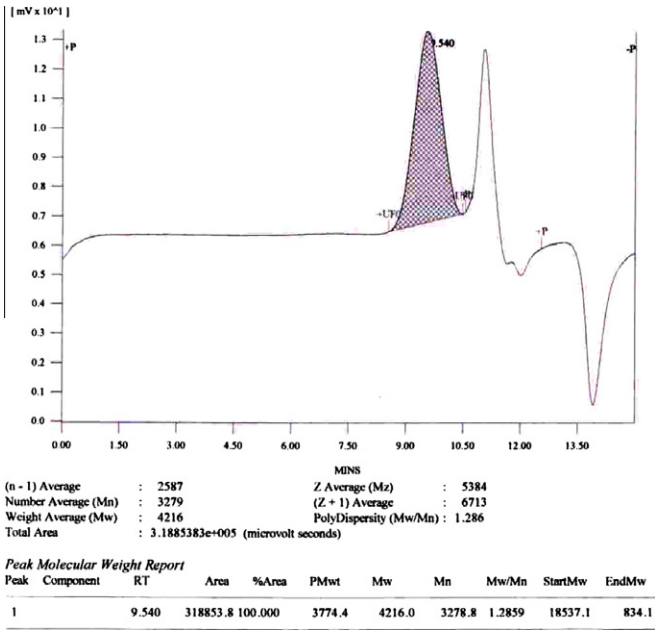

Fig. 8. GPC chromatogram PBCA NPs. (For interpretation of the references to colour in this figure legend, the reader is referred to the web version of this article.)

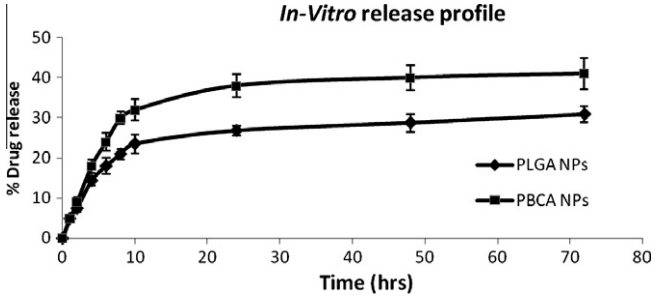

Fig. 9. *In vitro* release profile of PLGA and PBCA NPs.

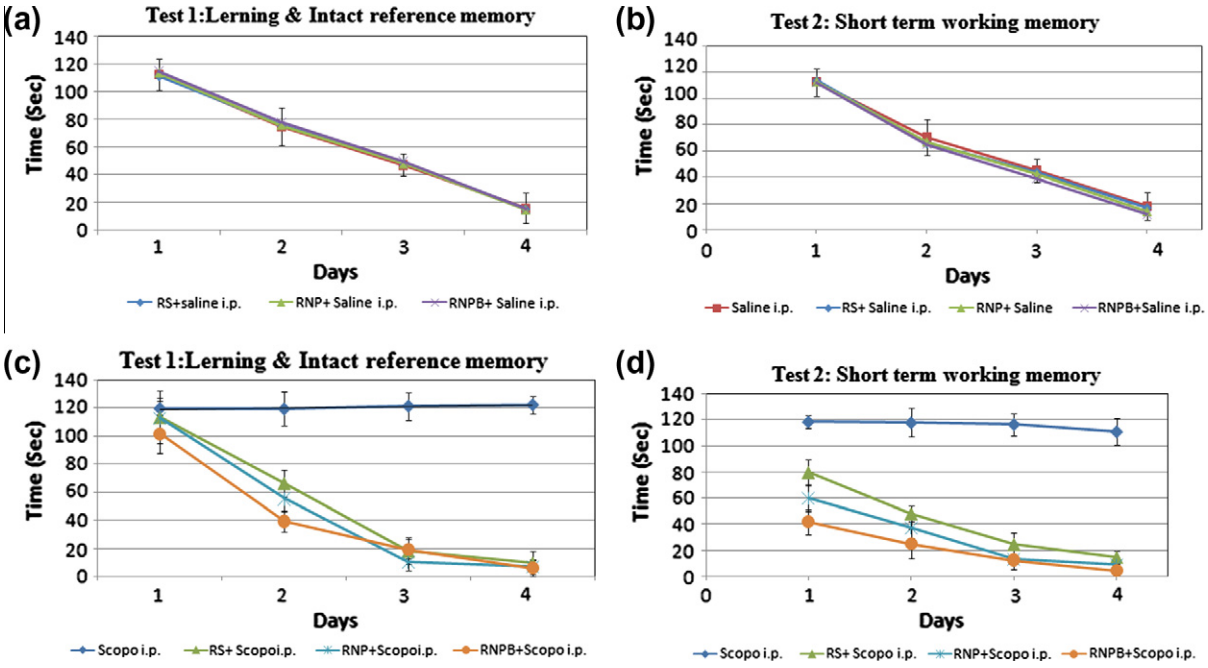

Fig. 10. *Saline-treated mice*: (a) Test 1: learning and intact reference memory, (b) Test 2: short-term working memory. ($n = 4$); *scopolamine-treated mice*: (c) Test 1: learning and intact reference memory, and (d) Test 2: short-term working memory. ($n = 4$). (For interpretation of the references to colour in this figure legend, the reader is referred to the web version of this article.)

was slow compared to intravenous injection of nanoparticulate formulations, and mice did not learn to reach platform even after 4 days. Thus, the results suggest faster memory regain in scopolamine-induced amnesic mice following intravenous injection of PLGA NPs and PBCA NPs, indicating effectiveness of both NPs in spatial memory improvement and behavioral acquisition in amnesic mice.

5. Conclusion

RT-loaded PLGA and PBCA NPs were prepared using modified nanoprecipitation method and emulsion polymerization method, respectively, with narrow size distribution (<200 nm) and higher entrapment efficiency. The study demonstrated the role of factorial design, derived reduced polynomial equation, contour plots and response surface plots in optimizing formulation variables affecting PS and PDE of prepared NPs. Using the factorial design, we could achieve a minimum PS together with maximum PDE with less number of experiments and could predict the PS and PDE for various combinations of the formulation variables using the contour plots and response surface plots. *In vitro* release was found to follow first-order Fickian diffusion kinetics in both PLGA and PBCA NPs. The release of RT from PLGA NPs was slower than PBCA NPs, which may be attributed to higher molecular weight of PLGA. Administration of RT formulations in saline-treated animals did not result in any noticeable improvement in learning and memory capacities, whereas administration of different RT-loaded NPs in scopolamine-treated mice antagonized the scopolamine-induced amnesia as evidenced by significant decrease ($P < 0.05$) in escape latency. These results indicated that compared to RT solution, PLGA and PBCA NPs resulted in faster memory regain in scopolamine-induced amnesic mice. These preliminary results indicate that RT-loaded PLGA and PBCA NP could be effective in brain targeting and sustaining RT release for a prolonged period and could be a significant improvement for treating Alzheimer's disease. Further studies are needed to support the findings of pharmacodynamic studies and to confirm the performance of NPs *in vivo*.

Acknowledgment

The authors would like to thank Sun Pharma Advanced Research Centre (SPARC), Vadodara for providing gift sample of rivastigmine tartrate.

References

[1] K.L. Lanctoat, N. Herrmann, K.K. Yau, L.R. Khan, B.A. Liu, M.M. Loulou, T.R. Einarson, Efficacy and safety of cholinesterase inhibitors in Alzheimer's disease: a meta-analysis, Can. Med. Assoc. J. 169 (2003) 557–564.
[2] P. Autuono, J. Beyer, The burden of dementia. A medical and research perspective, Theor. Med. Bioethics 20 (1999) 3–13.
[3] I. Tamai, A. Tsuji, Drug delivery through the blood brain barrier, Adv. Drug Deliv. Rev. 19 (1996) 401–424.
[4] N. Bodor, L. Prokai, W.M. Wu, H.H. Farag, S. Jonnalagadda, M. Kawamura, J. Simpkins, A strategy for delivering peptides into the central nervous system by sequential metabolism, Science 257 (1992) 698–1700.
[5] D. Devineni, A. Klein-Szanto, J.M. Gallo, Tissue distribution of methotrexate following administration as a solution and as a magnetic microsphere conjugate in rats bearing brain tumors, J. Neurooncol. 24 (1995) 43–152.
[6] J. Huwyler, D. Wu, W.M. Pardridge, Brain delivery of small molecules using immunoliposomes, Proc. Natl. Acad. Sci. 93 (1996) 4164–4169.
[7] J. Kreuter, Nanoparticle systems for brain delivery of drugs, Adv. Drug Deliv. Rev. 47 (2001) 65–81.
[8] S.V. Vinogradov, T.K. Bronich, A.V. Kabanov, Nanosized cationic hydrogels for drug delivery: preparation, properties and interactions with cells, Adv. Drug Deliv. Rev. 54 (2002) 135–147.
[9] J. Kreuter, R.N. Alyautdin, D.A. Kharkevich, A.A. Ivanov, Passage of peptides through the blood–brain barrier with colloidal polymer particles (NPs), Brain Res. 674 (1995) 171–174.
[10] U. Schroeder, P. Sommerfeld, S. Ulrich, B.A. Sabel, Nanoparticle technology for delivery of drugs across the blood–brain barrier, J. Pharm. Sci. 87 (1998) 1305–1307.
[11] R.N. Alyautdin, V.E. Petrov, K. Langer, A. Berthold, D.A. Kharkevich, J. Kreuter, Delivery of loperamide across the blood–brain barrier with polysorbate 80-coated poly (butylcyanoacrylate) nanoparticles, Pharm. Res. 14 (1997) 325–328.
[12] R.N. Alyautdin, E.B. Tezikov, P. Ramge, D.A. Kharkevich, D.J. Begley, J. Kreuter, Significant entry of tubocurarine into the brain of rats with polysorbate 80-coated poly(butylcyanoacrylate) nanoparticles: an in situ brain perfusion study, J. Microencapsul. 15 (1998) 67–74.
[13] A. Friese, E. Seiller, G. Quack, B. Lorenz, J. Kreuter, Increase of the duration of the anticonvulsive activity of a novel NMDA receptor antagonist using

poly(butylcyanoacrylate) nanoparticles as a parenteral controlled release system, Eur. J. Pharm. Biopharm. 49 (2000) 03–109.
[14] A.E. Gulyaev, S.E. Gelperina, I.N. Skidan, A.S. Antropov, G.Y. Kivman, J. Kreuter, Significant transport of doxorubicin into the brain with polysorbate 80-coated nanoparticles, Pharm. Res. 16 (1999) 1564–1569.
[15] J. Panyam, M.P. Dhali, S.K. Sahoo, W. Ma, S.S. Chakravarthi, G.L. Amidon, R.J. Levy, V. Labhasetwar, Polymer degradation and in vitro release of a model protein from poly (D, L-lactide-co-glycolide) nano- and micro-particles, J. Control. Rel. 92 (2003) 173–187.
[16] J.M. Anderson, M.S. Shive, Biodegradation and biocompatibility of PLA and PLGA microspheres, Adv. Drug Deliv. Rev. 28 (1997) 5–24.
[17] S. Sehra, A.S. Dhake, Formulation and evaluation of sustained release microspheres of poly-lactide-co-glycolide containing tamoxifen citrate, J. Microencaps. 22 (8) (2005) 521–528.
[18] J.M. Barichello, M. Morishita, K. Takayama, T. Nagai, Encapsulation of hydrophilic and lipophilic drugs in PLGA nanoparticles by the nanoprecipitation method, Drug Develop. Ind. Pharm. 25 (4) (1999) 471–476.
[19] K. Avgoustakis, Pegylated poly(lactide) and poly(lactide-co-glycolide) nanoparticles: preparation, properties and possible applications in drug delivery, Curr. Drug Del. 1 (2004) 321–333.
[20] Y. Jiao, N. Ubrich, M. Marchand-Arvier, C. Vigneron, M. Hoffman, T. Lecompte, P. Maincent, In vitro and in vivo evaluation of oral heparin–loaded polymeric nanoparticles in rabbits, Circulation 105 (2002) 230–235.
[21] C. Fonseca, S. Simões, R. Gaspar, Paclitaxel-loaded PLGA nanoparticles: preparation, physicochemical characterization and in vitro anti-tumoral activity, J. Control. Rel. 83 (2) (2002) 273–286.
[22] Z. Panagi, A. Beletsi, G. Evangelatos, E. Livaniou, D.S. Ithakissios, K. Avgoustakis, Effect of dose on the biodistribution and pharmacokinetics of PLGA and PLGA–mPEG nanoparticles, Int. J. Pharm. 221 (1–2) (2001) 143–152.
[23] I. Bala, S. Hariharan, M.N.V. Ravi Kumar, PLGA nanoparticles in drug delivery: the state of the art, Crit. Rev. Ther. Drug. Carriers 21 (2004) 387–422.
[24] F. Lescure, C. Zimmer, D. Roy, P. Couvreur, Optimization of polycyanoacrylate nanoparticle preparation: influence of sulfur dioxide and pH on nanoparticles characteristics, J. Colloid Interface Sci. 154 (1992) 77–86.
[25] F.M. Eskander, N.G. Nagykery, E.Y. Leung, B. Khelghati, C. Geula, Rivastigmine is a potent inhibitor of acetyl- and butyryl-cholinesterase in Alzheimer's plaques and tangles, Brain Res. 1060 (2005) 144–152.
[26] J. Vandervoort, A. Ludwig, Preparation factors affecting the properties of polylactide nanoparticles: a factorial design study, Pharmazie 56 (2001) 484–488.
[27] B. Singh, N. Ahuja, Development of controlled-release buccoadhesive hydrophilic matrices of diltiazem hydrochloride: optimization of bioadhesion, dissolution, and diffusion parameters, Drug Dev. Ind. Pharm. 28 (2002) 431–442.
[28] M.K. Dhiman, P.D. Yedurkar, K.K. Sawant, Buccal bioadhesive delivery system of 5-fluorouracil: optimization and characterization, Drug Dev. Ind. Pharm. 34 (2008) 761–770.
[29] S.B. Patil, K.K. Sawant, Development, optimization and in vitro evaluation of alginate mucoadhesive microspheres of carvedilol for nasal delivery, J. Microencaps. 26 (5) (2009) 432–443.
[30] T. Govender, S. Stolnik, M.C. Garnett, L. Illum, S.S. Davis, PLGA nanoparticles prepared by nanoprecipitation: drug loading and release studies of a water soluble drug, J Control. Release 57 (1999) 171–185.
[31] U. Bilati, E. Allemann, E. Doelker, Development of a nanoprecipitation method intended for the entrapment of hydrophilic drugs into nanoparticles, Eur. J. Pharm. Sci. 25 (2005) 67–75.
[32] J. Kreuter, R.N. Alyautdin, D.A. Karkevich, B.A. Sabel, Drug targeting to the nervous system by nanoparticles, US Patent 6 (117) (2000) 454.
[33] L.R. Harivardhan, R.S.R. Murthy, Influence of polymerization technique and experimental variables on the particle properties and release kinetics of methotrexate from poly (butylcyanoacrylate) nanoparticles, Acta Pharm. 54 (2004) 103–118.
[34] Y.B. Huang, Y.H. Tsai, S.H. Lee, J.S. Chang, P.C. Wu, Optimization of pH-independent release of nicardipine hydrochloride extended-release matrix tablets using response surface methodology, Int. J. Pharm. 289 (2005) 87–95.
[35] K. Adinarayana, P. Ellaiah, Response surface optimization of the critical medium components for the production of alkaline protease by a newly isolated Bacillus sp., J Pharm. Pharmaceut. Sci. 5 (3) (2002) 281–287.
[36] S. Akhnazarova, V. Kafarov, Experiment Optimization in Chemistry and Chemical Engineering, Mir publications, Moscow, 1982. pp. 18–94.
[37] C. Narendra, M.S. Srinath, B. Prakash Rao, Development of three layered buccal compact containing metoprolol tartrate by statistical optimization technique, Int. J. Pharm. 304 (2005) 102–114.
[38] N. Behan, C. Birkinshaw, N. Clarke, Poly n-butyl cyanoacrylate nanoparticles: a mechanistic study of polymerization and particle formation, Biomaterials 22 (2001) 1335–1344.
[39] N. Behan, C. Birkinshaw, Preparation of poly(butyl cyanoacrylate) nanoparticles by aqueous dispersion polymerization in the presence of insulin, Macromol. Rapid Commun. 22 (2001) 41–43.
[40] Y. Hu, X. Jiang, Y. Ding, L. Zhang, C. Yang, J. Zhang, J. Chen, Y. Yang, Preparation and drug release behaviors of nimodipine-loaded poly(caprolactone)–poly(ethylene oxide)–polylactide amphiphilic copolymer nanoparticles, Biomaterials 24 (2003) 2395–2404.
[41] H. Ge, Y. Hu, X. Jiang, D. Cheng, Y. Yuan, H. Bi, C. Yang, Preparation, characterization, and drug release behaviors of drug nimodipine-loaded poly(ε-caprolactone)–poly(ethylene oxide)–poly(ε-caprolactone) amphiphilic triblock copolymer micelles, J. Pharm. Sci. 91 (2002) 1463–1473.
[42] R.G. Morris, Developments of a water-maze procedure for studying spatial learning in the rat, J. Neurosci. Meth. 11 (1984) 47–60.
[43] V. Jogani, P. Shah, A. Mishra, P. Mishra, A. Misra, Intranasal mucoadhesive microemulsion of tacrine to improve brain targeting, Alzheimer Dis. Assoc. Disord. 22 (2) (2008) 116–124.
[44] S. Bolton, C. Bon, Pharmaceutical Statistics: Practical and Clinical Applications, third ed., Marcel Dekker Inc., New York, 1997. pp. 562–563.
[45] G.E.P. Box, W.G. Hunter, J.S. Hunter, Statistics for Experiments, John Wiley and Sons, New York, 1978. pp. 291–334.
[46] W.G. Cochran, G.M. Cox, Experimental Designs, second ed., John Wiley and Sons, New York, 1992. pp. 335–375.
[47] F. Gabor, B. Ertl, M. Wirth, R. Mallinger, Ketoprofen poly (D, L-lactic-co-glycolic acid) microspheres: influence of manufacturing parameters and type of polymer on the release characteristics, J. Microencaps. 16 (1) (1999) 1–12.
[48] A. Zimmer, J. Kreuter, J. Robinson, Studies on the transport pathway of PBCA nanoparticles in ocular tissues, J. Microencaps. 8 (4) (1991) 497–504.
[49] S. Feng, G. Huang, Effects of emulsifiers on the controlled release of paclitaxel (Taxol) from nanospheres of biodegradable polymers, J. Control. Release. 71 (2001) 53–69.
[50] http://www.accessdata.fda.gov/drugsatfda_docs/label/2006/020823s016,021025s008lbl.
[51] B. Wilson, M.K. Samanta, K. Santhi, K.P. Sampath kumar, N. Paramkrishna, B. Suresh, Poly(n-butylcyanoacrylate) nanoparticles coated with polysorbate 80 for the targeted delivery of Rivastigmine into the brain to treat Alzheimer's disease, Brain Res. 1200 (2008) 159–168.
[52] J. Duan, Y. Zhang, W. Chen, C. Shen, M. Liao, Y. Pan, J. Wang, X. Deng, J. Zhao, Cationic polybutyl cyanoacrylate nanoparticles for dna delivery, J. Biomed. Biotech. (2009) 149254.
[53] A.C. Yang, H. Ge Xiong, H. Yong, X.Q. Jiong, C.Z. Yang, Doxorubicin loaded poly (butylcyanoacrylate) nanoparticles produced by emulsifier free emulsion polymerization, J. Appl. Polym. Sci. 78 (2000) 517–526.
[54] M. Dunne, O. Corrigan, Z. Ramtoola, Influence of particle size and dissolution condition on the degradation properties of polylactide-co-glycolide particles, Biomaterials 21 (2000) 1659–1668.
[55] O.I. Corrigan, Xue Li, Quantifying drug release from PLGA nanoparticulates, Euro. J. Pharm. Sci. 37 (3–4) (2009) 477–485.
[56] C.Y. Huang, Y.D. Lee, Core-shell type of nanoparticles composed of poly[(n-butyl-cyanoacrylate)-co-(2-octyl-cyanoacrylate)] copolymers for drug delivery application: synthesis, characterization and in vitro degradation, Int. J. Pharm. 325 (2006) 132–139.
[57] O.I. Corrigan, Xue Li, Quantifying drug release from PLGA nanoparticles, Euro. J. Pharm. Sci. 37 (3–4) (2009) 477–485.